

# INFLUENCE OF ERRORS ON THE ESRF UPGRADE LATTICE

S.M. Liuzzo, J.C. Biasci, N. Carmignani, L. Farvacque, G. Gatta, G. Le Bec, D. Martin, B. Nash, T. Perron, P. Raimondi, R. Versteegen, S. White, ESRF, Grenoble, France

## Abstract

To determine the tolerable alignment and magnetic errors for the ESRF upgrade, we study their influence on Touschek lifetime and dynamic aperture. The correction of each set of errors studied is performed with a commissioning-like procedure, from the search for a closed orbit to the correction of resonance driving terms. Each kind of error is studied independently for each relevant family of magnets. The tolerable values deduced from the analysis are within the practical limits. The impact of the measured and simulated survey errors is also considered, defining the position of the currently installed lattice as the one of least impact for the realignment of X-ray beamlines.

## INTRODUCTION

The ESRF Phase II Upgrade storage ring will replace the present light source in 2020, increasing the X-rays brilliance by a factor 40 providing 5% of coherence (at 1 keV) [1]. The chosen lattice for the upgrade is a Hybrid Multi Bend Achromat (HMBA) lattice, with theoretical equilibrium horizontal emittance of 134 pmrad. This lattice is depicted in Fig.1 and features a 32 fold symmetry. The symmetry is broken at the injection straight section to allow for higher beta-functions at the injection point. This insertion has effects on lifetime and dynamic aperture shown in [2]. The sextupoles are lo-

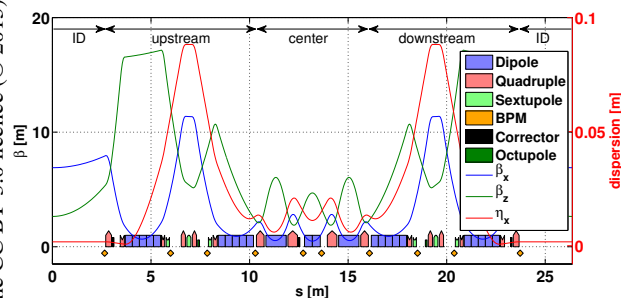


Figure 1: ESRF upgrade unit lattice cell (HMBA).

cated in high dispersion and beta regions (dispersion bumps) and with an almost perfect -I transformation between the first three and last three sextupoles. This allows to cancel the second order sextupolar effects [3]. To enforce this condition in the limited space of the cell, two families of high gradient (91 T/m) focusing quadrupoles (QF6/8) are included together with combined function dipoles (DQ) [4]. To achieve these large fields a smaller bore radius is required and the vertical apertures in the central region of the lattice are reduced to 6.5 mm (10 mm in the rest of the cell). This small aperture and the phase space distortion between the sextupoles lead to strong error sensitivity in this region, mitigated by the smaller equilibrium beam size. To optimize the emittance of the lattice, the first and last two dipoles used in

the cell have a longitudinal gradient (DL). In addition one family of octupoles is used to adjust the horizontal detuning with amplitude.

In this paper we look at the influence of alignment and field errors on lifetime, dynamic aperture and injection efficiency for all the magnets (version S28).

## Errors Modeling

The coordinate system used in this document follows the trajectory of the reference orbit. The errors studied for dipoles, quadrupoles, sextupoles, octupoles and girders (support of magnet groups) are:

- transverse displacements  $\Delta x$  (radial) and  $\Delta y$  (vertical)
- longitudinal displacements  $\Delta s$
- rotation about the beam direction  $\Delta\psi$
- integral field errors  $\frac{\Delta K_0}{K_0}, \frac{\Delta K_1}{K_1}, \frac{\Delta K_2}{K_2}, \frac{\Delta K_3}{K_3}$
- multipole errors (random and systematic)
- survey errors (random and systematic)

The DL dipoles and DQ dipoles are modeled in the lattice using several separated dipoles. The errors set in these magnets take in account this modeling choice and move the DLs and DQs slices as single magnets. Girder displacements are simulated by systematic movements of all magnets on the same girder. Beam position monitors (BPM) are displaced following the girders. Rotations of the dipoles are included as errors and do not affect the reference orbit.

## Lattice Tuning and Correction

Simulations are done using the Accelerator Toolbox [5]. The errors are set for the desired magnet and the correction is performed with all the available correctors in the lattice: three dedicated correctors and six sextupoles with coils for horizontal and vertical steering and skew quadrupole correction. After the application of a procedure to find the closed orbit, the correction is performed following the techniques used in operation for the present accelerator: correction of tunes, orbit, normal and skew quadrupole resonance driving terms [6] and finally chromaticities. The procedure is iterated until convergence. Additional sextupole and octupole corrections are under investigation, together with many other algorithms, to be able to exploit all the available tuning knobs. The final parameters after correction are: rms orbits of  $\sim 100 \mu\text{m}$ , rms dispersion  $< 1 \text{ mm}$  in the horizontal plane and  $\sim 200 \mu\text{m}$  in the vertical plane,  $< 1 \%$   $\beta$ -beating in both planes and the an emittance ratio of  $\sim 0.1 \%$ . The required correctors strengths are within the power supply limits.

## IMPACT OF ERRORS

The conditions to be achieved for a lattice with errors are:

- at least 8 mm of dynamic aperture towards the inner

Content from this work may be used under the terms of the CC BY 3.0 licence (© 2015). Any distribution of this work must maintain attribution to the author(s), title of the work, publisher, and DOI.

side of the ring for off-axis injection, including the septum thickness and  $3\sigma$  beam stay clear,

- emittances not exceeding 4 pmrad variation in both planes after correction,
- as large as possible lifetimes.

To compute lifetime (0.2 mA/bunch) and injection efficiency the vertical emittance is set to 5 pmrad (to be achieved with white noise or coupling). The injection efficiency is computed considering a round 30 nmrad Gaussian beam injected with horizontal beta functions matched to be equal to half the beta function at the injection septum (an approximation of to the optimal value found in [7]) in the storage ring. This analysis is performed using the ESRF computing cluster.

### Alignment and Main Field Errors

To determine the tolerable values, the orbit, dispersion,  $\beta$ -beating, emittance, dynamic aperture and lifetime are evaluated (after correction) for increasing random error amplitudes. The random errors are drawn from a truncated Gaussian distribution ( $2\sigma$ ), and applied to each relevant magnet group. In Fig.2 each curve represents the Touschek lifetime averaged over ten seeds of errors for a defined group of magnets and error kind (the range is shown in the legend). Various information concerning random errors tolerances

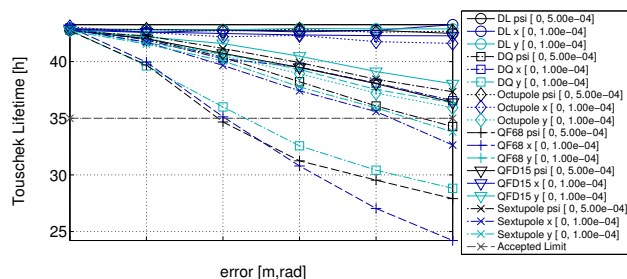


Figure 2: Touschek lifetime after correction as a function of error amplitude for various errors and magnets (the error ranges are reported in the legend).

can be deduced from Fig.2. The alignment errors of DQ, QF6 and QF8 quadrupoles (the center region of the unit cell, see Fig.1) are the ones with the strongest impact on the reduction of lifetime. Sextupoles have significant impact as well, while a limited reduction of lifetime is observed in the studied error ranges for moderate gradient quadrupoles, longitudinal gradient dipoles and octupoles. However, the misalignment of these magnets has a relevant impact on dynamic aperture. Taking into account each error individually and each relevant group of magnets it is possible to estimate the tolerable errors [8]. To consider the simultaneous impact of several errors in the determination of the tolerated values, the individual errors are allowed to reduce lifetime to 35 h and dynamic aperture to 10 mm (the required values are  $D.A. > 8$  mm,  $\tau > 20$  h). The tolerable errors of alignment and main field component are listed in Table 1. The tolerable error between two consecutive magnets is in the worst case  $\sqrt{2} \cdot 50 \mu\text{m}$ . Considering the error on the fiducialization

Table 1: Tolerable Alignment and Main Multipole Field Gradient Errors. Estimated to provide 8 mm dynamic aperture at septum for off axis injection and lifetime of about 20 h.

errors	$\Delta x$	$\Delta y$	$\Delta\psi$	$\Delta s$	$\Delta K_n/K_n$
units	$\mu\text{m}$	$\mu\text{m}$	$\mu\text{rad}$	$\mu\text{m}$	
DL	100	100	500	1000	$10 \cdot 10^{-4}$
DQ	70	50	200	1000	$5 \cdot 10^{-4}$
QDF15	100	85	200	1000	$5 \cdot 10^{-4}$
QF68	50	70	200	1000	$5 \cdot 10^{-4}$
Sextupole	70	50	500	1000	$35 \cdot 10^{-4}$
Octupole	100	100	500	1000	$50 \cdot 10^{-4}$

(magnet-axis to survey monuments,  $28 \mu\text{m}$ ), the magnet position measurement error ( $20 \mu\text{m}$ ) and the alignment network error ( $49 \mu\text{m}$ ) these tolerances are achievable.

**Girder errors** There are four 5.1 m long girders in each cell. The estimated tolerable misalignment is  $50 \mu\text{m}$  rms horizontal and vertical, governed again by the misalignment of the central region girders. This value is not included in the list of tolerable errors, since the achievement of the above stated errors (Table 1) for the individual magnets will also grant the alignment of the girder to this precision. Moreover, the simulations of survey errors give a more relevant information concerning the positioning tolerances of girders.

### Multipole Errors

The initial estimation of tolerable multipole field errors has been performed generating random allowed multipole field errors that would provide a predetermined field error at the limit of the good field region ( $\Delta B/B|_{r_0}$ ,  $\Delta G/G|_{r_0}, \dots$ ). Studying the impact on dynamic aperture and lifetime, the

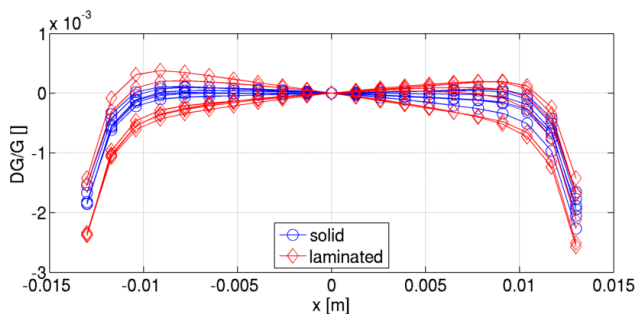


Figure 3: Example of multipole errors (random and systematic) estimated from the magnetic design of QD2 magnets. The curves are shown for the case of laminated and solid iron design.

tolerable limit has been provided to the magnet design group. The design of the magnet has then been finalized, achieving multipole errors well within the tolerances. The multipole errors obtained by 2D analysis of the magnetic field at the

Content from this work may be used under the terms of the CC BY 3.0 licence (© 2015). Any distribution of this work must maintain attribution to the author(s), title of the work, publisher, and DOI.

nominal current for all magnet families have been used to estimate the impact on dynamic aperture and lifetime. Random multipoles introduced by pole misplacement and machining tolerances have also been defined in the case of laminated ( $\pm 40 \mu\text{m}$ ) or solid iron ( $\pm 20 \mu\text{m}$ ) magnets. As an example, in Fig.3 the multipole field errors for the QD2 quadrupoles are reported. Multipole errors have a limited impact on dynamic aperture and lifetime (Table 2) compared to random errors, allowing for relaxed machining tolerances. The dipole and quadrupole multipole components have been ignored as it is possible to correct them using steerers and independent quadrupole power supplies.

### Survey Errors

After more than twenty years of operation the ESRF storage ring has slowly moved to the position depicted in Fig. 4 [9], measured during the latest survey campaign. The ef-

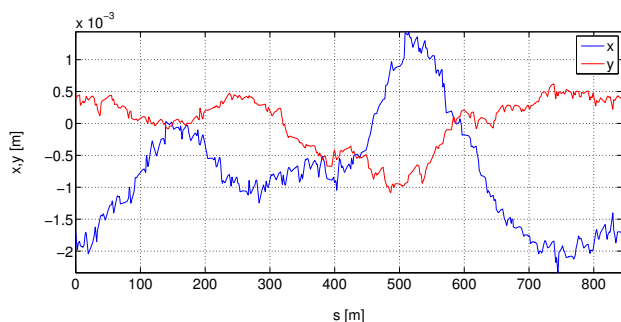


Figure 4: Survey of the ESRF storage ring positions in 2014.

fects of this large smooth excursion is limited as the errors between consecutive magnets are small. The position of the future storage ring has been simulated for many error seeds considering the present measurement errors and alignment procedure, for two cases: for a storage ring placed on the present position (actual survey) or back on the circular zero reference (nominal survey). The impact of this smooth displacement of the storage ring is shown in Table 2.

**X-ray at beamlines** The X-ray beamlines are aligned according to the actual position of the accelerator. The possibility of realigning the accelerator on the nominal position is under discussion. Figure 5 shows the position of the X-ray beam at the beamlines detectors (about 60 m after the source point) for the two possible repositioning. Even if possible, the realignment to the nominal position would require stronger corrections or girder movements with an impact on the commissioning time. However this operation could be anticipated using the current lattice. The installation of the lattice in the nominal position would be of less impact on lifetime, as shown in Table 2.

## CONCLUSIONS

The lifetime, dynamic aperture and injection efficiency arising from the errors described above are listed in Table 2 in ascending order. Random alignment and main field errors

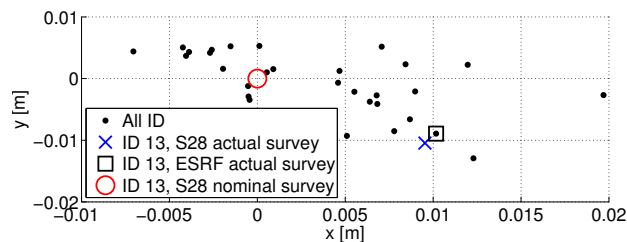


Figure 5: Position of the X-ray beam at the experiment (60 m after the source) for the ESRF storage ring considering the survey position and random errors.

Table 2: Dynamic Aperture at Septum, Lifetime and Injection Efficiency for Various Error Sources Averaged over 10 Seeds. Random refers to alignment and main field error.

error	DA (mm)	$\tau_{Tou.}$ (h)	Inj. eff. (%)
none	-13.1	45.1	100
solid (1)	$-12.9 \pm 0.1$	$43.4 \pm 0.8$	100
laminated (2)	$-12.5 \pm 0.1$	$40.5 \pm 1.7$	100
nominal survey (3)	$-11.3 \pm 0.3$	$41.4 \pm 1.6$	100
actual survey (4)	$-11.3 \pm 0.3$	$32.3 \pm 0.7$	100
random (Table 1) (5)	$-10.9 \pm 0.8$	$26.1 \pm 2.1$	$99.5 \pm 0.8$
(2+4+5) 50 seeds	$-10.7 \pm 1.1$	$23.5 \pm 1.8$	$95.6 \pm 3.6$

are taken from the list of tolerable errors in Table 1, survey errors and multipole errors are provided by the magnetic design and from alignment survey simulations. Figure 6 shows the on energy dynamic apertures for fifty seeds in the case where all sources are considered simultaneously (laminated magnets and actual survey): the lifetime and the injection efficiency are dominated by random errors (see Table 2).

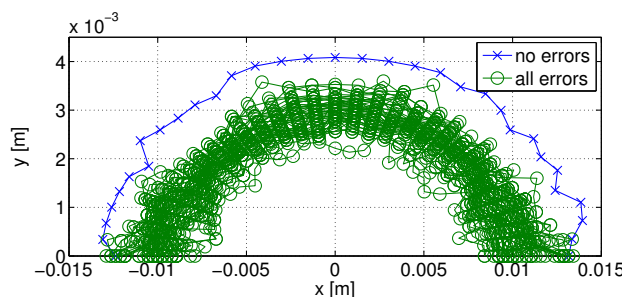


Figure 6: Dynamic aperture for 50 seeds of errors. Without errors (blue), and with random errors, survey errors about the actual position and multipole field errors for laminated magnets (green). Tracking is performed over 512 turns.

The average final values are within the required limits and the error values used to evaluate them are compatible with the mechanical, magnetic and alignment tolerances.

## REFERENCES

- [1] Biasci, J.C. et al., “A low emittance lattice for the ESRF”, *Synchrotron Radiation News*, vol. 27, Iss.6, 2014.
- [2] Carmignani, N. et al., “Linear and nonlinear optimizations for the ESRF upgrade lattice”, *TUPWA013, These Proceedings, IPAC’15, Richmond, Virginia, USA (2015)*.
- [3] Wiedemann, H., *Particle accelerator physics*, Volume II, p. 140, sec. ed., 1998.
- [4] Le Bec, G. et al., “Shape optimization for the ESRF II magnets”, *TUPRO082, IPAC14, Dresden, Germany, 2014*.
- [5] Nash, B. et al., “New functionality for beam dynamics in Accelerator Toolbox (AT)”, *MOPWA014, These Proceedings, IPAC’15, Richmond, Virginia, USA (2015)*.
- [6] Franchi, A. et al., “Vertical emittance reduction and preservation in electron storage rings via resonance driving terms correction”, *Phys. Rev. ST Accel. Beams*, 14:034002, Mar 2011.
- [7] Streun, A., “SLS booster-to-ring transferline optics for optimum injection efficiency”, *SLS-TME-TA-2002-0193 (2005)*.
- [8] Liuzzo, S.M., “Optimization Studies and measurements for ultra low emittance lattices”, PhD Thesis, University of Roma Tor Vergata, 2013.
- [9] Martin, D. et al., “Some design considerations for the ESRF upgrade program experimental hall slab”, *IWAA, DESY Hamburg, 2010*.